

Article

Climatic Warming-Induced Drought Stress Has Resulted in the Transition of Tree Growth Sensitivity from Temperature to Precipitation in the Loess Plateau of China

Qindi Zhang ¹ , Shaomin Fu ¹, Hui Guo ¹, Shaoteng Chen ^{2,3} and Zongshan Li ^{2,4,*}

¹ College of Life Sciences, Shanxi Normal University, Taiyuan 030031, China; nyzqd@126.com (Q.Z.); fuuu1999@163.com (S.F.); ghfsmzlh@163.com (H.G.)

² State Key Laboratory of Urban and Regional Ecology, Research Center for Eco-Environmental Science, Chinese Academy of Sciences, Beijing 100085, China; chtcst@163.com

³ Institute of International Rivers and Eco-Security, Yunnan University, Kunming 650500, China

⁴ National Observation and Research Station of Earth Critical Zone on the Loess Plateau in Shaanxi, Xi'an 710061, China

* Correspondence: zsli_st@rcees.ac.cn; Tel.: +86-152-0115-7915

Simple Summary: Although two warming phases have been confirmed over the past century, the responses of tree growth in drylands remain uncertain. To investigate this, we utilized the tree-ring chronology in the Loess Plateau of China to explore the changes in tree growth–climate relationships during these warming phases. Our findings indicate that tree growth rates primarily increased during the first warming phase (1910–1940) and decreased during the second phase (1970–2000). Furthermore, we observed that temperature was the main influencing factor for tree growth during the first phase, whereas drought played a more significant role during the second phase. These temporal changes emphasize the importance of water availability for tree growth in drylands and suggest that reductions in precipitation will further exacerbate the adverse effects of climate warming on tree growth.



Citation: Zhang, Q.; Fu, S.; Guo, H.; Chen, S.; Li, Z. Climatic Warming-Induced Drought Stress Has Resulted in the Transition of Tree Growth Sensitivity from Temperature to Precipitation in the Loess Plateau of China. *Biology* **2023**, *12*, 1275. <https://doi.org/10.3390/biology12101275>

Academic Editor: De Li Liu

Received: 26 August 2023

Revised: 22 September 2023

Accepted: 23 September 2023

Published: 25 September 2023



Copyright: © 2023 by the authors. Licensee MDPI, Basel, Switzerland. This article is an open access article distributed under the terms and conditions of the Creative Commons Attribution (CC BY) license (<https://creativecommons.org/licenses/by/4.0/>).

Abstract: Ongoing climate warming poses significant threats to forest ecosystems, particularly in drylands. Here, we assess the intricate responses of tree growth to climate change across two warming phases (1910–1940 and 1970–2000) of the 20th century in the Loess Plateau of China. To achieve this, we analyzed a dataset encompassing 53 ring-width chronologies extracted from 13 diverse tree species, enabling us to discern and characterize the prevailing trends in tree growth over these warming phases. The difference in the primary contributors over two warming phases was compared to investigate the association of tree growth with climatic drivers. We found that the first warming phase exerted a stimulating effect on tree growth, with climate warming correlating to heightened growth rates. However, a contrasting pattern emerged in the second phase as accelerated drought conditions emerged as a predominant limiting factor, dampening tree growth rates. The response of tree growth to climate changed markedly during the two warming phases. Initially, temperature assumed a dominant role in driving the tree growth of growth season during the first warming phase. Instead, precipitation and drought stress became the main factors affecting tree growth in the second phase. This drought stress manifested predominantly during the early and late growing seasons. Our findings confirm the discernible transition of warming-induced tree growth in water-limited regions and highlight the vulnerability of dryland forests to the escalating dual challenges of heightened warming and drying. If the warming trend continues unabated in the Loess Plateau, further deterioration in tree growth and heightened mortality rates are foreseeable outcomes. Some adaptive forest managements should be encouraged to sustain the integrity and resilience of these vital ecosystems in the Loess Plateau and similar regions.

Keywords: climate change; tree radial growth; Loess Plateau; warming phases

1. Introduction

The Fifth Assessment Report of the Intergovernmental Panel on Climate Change (IPCC AR5) states that the world experienced two distinct warming phases during the 20th century [1]. The early part of the 20th century (1910–1940) exhibited a clear warming trend in global temperatures (the first warming phases hereafter). In the second half of the 20th century (1970–2000), global temperatures once again rose significantly (the second warming phase hereafter). The impact of climate change, notably in drylands, reverberates acutely across forest ecosystems due to the inherent intricacies of tree longevity, which constrains swift adaptation to energy and water constraints [2,3]. Climate warming impacts the health and functioning of dryland forest ecosystems with consequences on substantial ecosystem services for human well-being, including water and soil conservation as well as carbon sequestration and climate change mitigation [4–6]. Climate projections suggest that increases in temperature across the boreal forest region are likely to exceed 2 °C by the end of the century [7]. Climate warming in the future will bring great uncertainty to the forest dynamics. Therefore, understanding the potential effects of climate warming on forest ecosystems is a long-standing goal of the forest ecological research agenda in water-limited regions.

Rising temperatures have multifaceted effects on plants, including increased energy inputs, an elevated vapor-pressure deficit, and decreased soil moisture [8]. Tree radial growth has strong connections to climate change. In this sense, tree ring indices provide higher-resolution information on tree growth response to changing climate [9]. Despite numerous dendroclimatological studies aimed at elucidating tree growth-climate relationships in water-limited regions, there persists considerable variability in forest responses to climate warming [10–12]. In general, elevated temperatures tend to foster growth in cool regions, such as the Tibetan Plateau [13–15]. However, it is important to note that beyond a certain temperature threshold, tree growth is adversely affected, primarily due to diminishing net photosynthetic gains [12]. Furthermore, as energy inputs increase, the influence of water availability on plant growth often surpasses that of the temperature [3]. Consequently, higher temperatures are generally associated with reduced tree growth in water-limited regions, culminating in diminished growth rates and an accelerated incidence of tree mortality [16–18]. Nevertheless, the confluence of climate warming also introduces a layer of uncertainty, encompassing shifts in precipitation patterns, storm intensity, drought frequency, and the severity of extreme events. The intricacies of plant growth are attributed to complex interactions between energy and water availability rather than a singular driver [19]. In the context of global warming, although it is appreciated that temperature always interacts with other factors in producing an effect, large uncertainties still remain around the relative importance of the climatic drivers of plant growth over time. This ambiguity is particularly pronounced in water-limited regions such as the Loess Plateau.

The Loess Plateau, situated in the arid and semi-arid region of Northwestern China, holds immense significance for soil-erosion control and vegetation restoration, playing a pivotal role in ecological security and development [20,21]. Over the past few decades, temperatures in this region have experienced a substantial increase, with a warming rate exceeding twice the Northern Hemisphere average [22]. Climate projections for the Loess Plateau augur a continued rise in temperatures throughout the plateau, with the northern and eastern regions prognosticated to undergo the most pronounced changes [23]. Against this backdrop, the objectives of the present study were to investigate how tree growth responds to climate variability across two warming phases. To achieve this, we amassed a dataset comprising 53 ring-width chronologies derived from 13 tree species native to the Loess Plateau, encompassing the two warming phases prevalent during the 20th century. Drawing from previous research, we formulated two hypotheses: (1) Climate warming has incurred a decline in tree growth, and (2) The climate drivers governing tree growth exhibit disparities between these two warming phases. To test these hypotheses, we initially scrutinized the trends in climate parameters and tree growth across the two

warming phases. Subsequently, we delved into the intricacies of the tree growth–climate relationships, discerning any alterations that transpired between the two phases.

2. Materials and Methods

2.1. Study Area

This study was conducted in the Loess Plateau of China (33.72°–41.27° N and 100.90°–114.55° E) (Figure 1). The average altitude is around 1000 m, decreasing from northwest to southeast. The Loess Plateau has a typical warm temperate continental monsoon climate. The mean annual temperature (MAT) exhibits regional variability, ranging from 3.6 °C in the northwest to 14.3 °C in the southeast. Mean annual precipitation (MAP) ranges from 123.3 mm in the northwest to 948.9 mm in the southeast [24]. More than 60% of precipitation falls between July and September. The vegetation distribution within this region displays a clear zonal pattern, with a diverse array of tree genera like *Pinus*, *Abies*, *Picea*, and *Larix* widely scattered throughout the forested areas owing to the intricate interplay between topography and climatic factors [25].

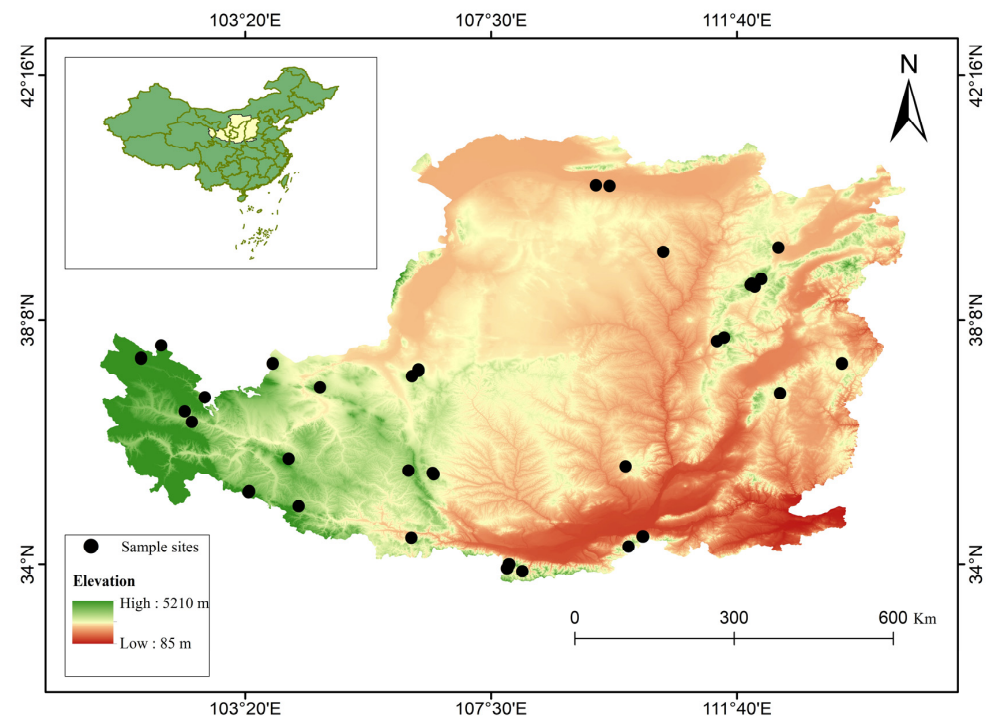


Figure 1. Distribution of sample sites of the Loess Plateau of China.

2.2. Chronological Data

The tree-ring width chronologies utilized in this study were exclusively derived from the Loess Plateau (Figure 1, Table S1). Initially, the tree-ring width chronologies specific to this region were sourced from the International Tree-ring Data Bank (ITRDB). Additionally, relevant studies pertaining to tree-ring analysis in the Loess Plateau were scanned and retrieved from Web of Science and the China National Knowledge Infrastructure (<https://www.cnki.net/>, accessed on 23 September 2022). These tree-ring data were subsequently digitized from graphical representations of the tree-ring chronologies using GetData software (v.2.26; <https://soft.3dmgame.com/download/167665.html>, accessed on 14 June 2022).

To ensure the integrity of the dataset for subsequent analyses, only tree-ring width chronologies adhering to the following criteria were retained: (a) Chronologies exhibiting total ring-width and (b) Chronologies encompassing both warming periods 1910–1940 and 1970–2000. After screening, 95 chronological series were preserved. Subsequently, 53 tree-ring width chronosequences with positive growth rates during the first warm-

ing phase were selected from the 95 sequences. Eventually, a total of 53 chronology series were deemed suitable for inclusion. These selected chronological series represent 13 species belonging to 7 genera. In order to compensate for inter-species variations and account for age-related growth patterns, all chronology series underwent normalization and standardization procedures.

2.3. Climate Data

We quantified the response of tree growth to three climate parameters: temperature, precipitation, and standardized precipitation evapotranspiration index (SPEI). The SPEI is an index that can be used as a measure of changing climate characteristics to describe long-term meteorological evapotranspiration increase and decrease trends. It can be used to measure changes in drought or flooding in an area to judge future changes in the area's water resources, with smaller SPEI values indicating a drier climate. These parameters were used as metrics of energy and water availability, and drought, respectively. The monthly temperature, precipitation, and SPEI data for each sampling site were obtained from the Climatic Research Unit (CRU) time series (TS) version 4.05, available at a $0.5 \times 0.5^\circ$ grid size. The data cover the period from 1900 to 2020 and can be accessed through the website <https://www.uea.ac.uk/web/groups-and-centres/climatic-research-unit/data> (accessed on 22 September 2023). To facilitate our analysis, we curated a 17-month dataset encompassing the period from the prior June to the current October. Within this dataset, we derived a 5-month sliding window, computing the average climate data.

2.4. Statistical Analysis

In this study, our primary objective is to comprehensively evaluate the disparities in tree radial growth characteristics and climate sensitivity within the Loess Plateau during two warming phases. To achieve this, we employed a range of statistical analyses. Firstly, linear regression was employed to discern the temporal trends of three climate factors: temperature, precipitation, and SPEI, as well as tree growth during the two warming periods. Then, Pearson correlation analysis was conducted to provide insights into the relationship between tree responses and climate sensitivity. Finally, paired-sample *t*-tests were utilized to explore the variability in the correlations of tree-ring index with temperature, precipitation, and SPEI across the months in the two warming phases. All of the above statistical tests were conducted using SPSS version 25.0 (IBM Corporation, New York, NY, USA).

3. Results

3.1. Trends in Climate and Tree Growth

In Figure 2, we present trends in climate and tree growth observed during two distinct warming phases in the Loess Plateau. MAT continued to rise steadily in both phases, from a value of 5.607 ± 0.206 °C in the first warming phase to 5.807 ± 0.232 °C in the second warming phase. MAP did not change significantly with time during the first warming phase, while it showed an insignificant decreasing trend during the second warming phase. SPEI showed a decreasing trend in both warming phases. Specifically, MAP decreased from 512.295 ± 0.226 mm to 510.902 ± 0.225 mm, while SPEI decreased from -0.039 ± 0.224 to -0.409 ± 0.240 . Tree growth rates exhibited divergent patterns during these warming phases (Figure 2d). In the first warming phase, there was a notable upward trend in overall tree growth rates ($p < 0.01$). However, in the second phase, tree growth rates demonstrated a significant downward trend ($p < 0.01$). The average tree growth rate increased from 0.027 ± 0.020 in the first warming phase to -0.016 ± 0.032 in the second phase (Table S2). With regards to individual tree species, the majority displayed an initial increase in growth rates followed by a subsequent decrease, with the exception of *Abies chensiensis* and *Abies fargesii* (Figure S1).

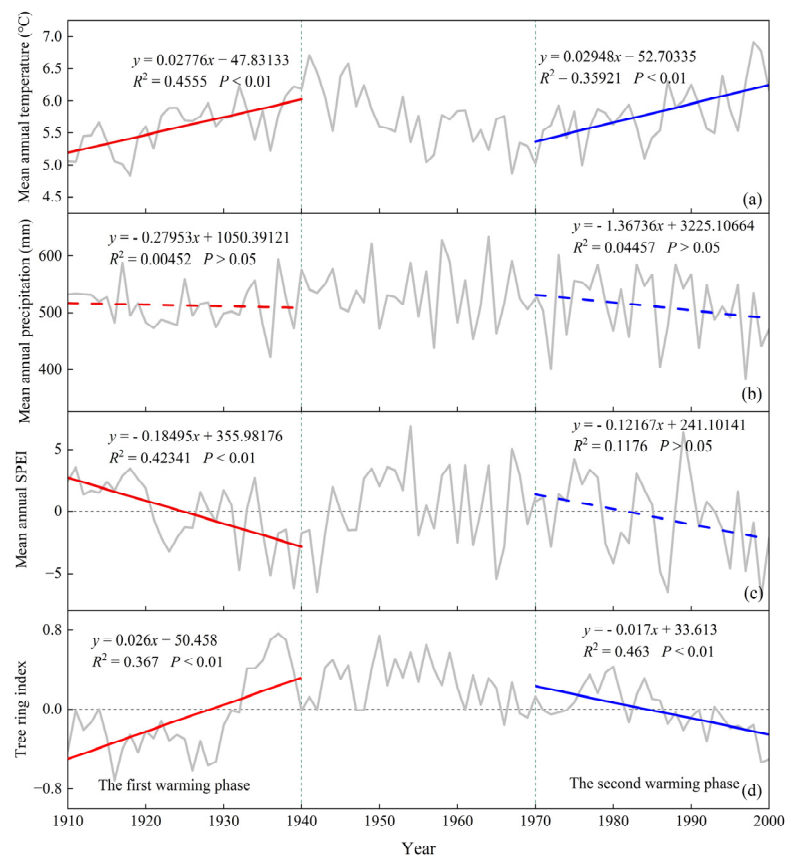


Figure 2. Climate change and tree growth trends in two warming phases. (a) Trends in the MAT; (b) Trends in the MAP; (c) Trends in the SPEI; (d) Trends in tree growth. The red trend line represents the fitted line of climate and tree growth rates for the first warming phase, while the blue colour similarly represents the second warming phase.

3.2. Spatial Pattern of Growth Rate and Climatic Sensitivity

Many of the tree ring sites that exhibited positive growth rates in the first warming phase transitioned to negative growth rates in the second phase (Figure 3a,b). The correlation between tree growth rates and MAT showed a spatially positive relationship in the first warming phase, which weakened significantly in the second phase (Figure 3c,d). Conversely, the response of tree growth rates to water availability (MAP and SPEI) considerably improved in the second warming phase (Figure 3f,h). Overall, the sensitivity of tree growth to climate shifted from temperature in the first warming phase to precipitation and SPEI in the second phase.

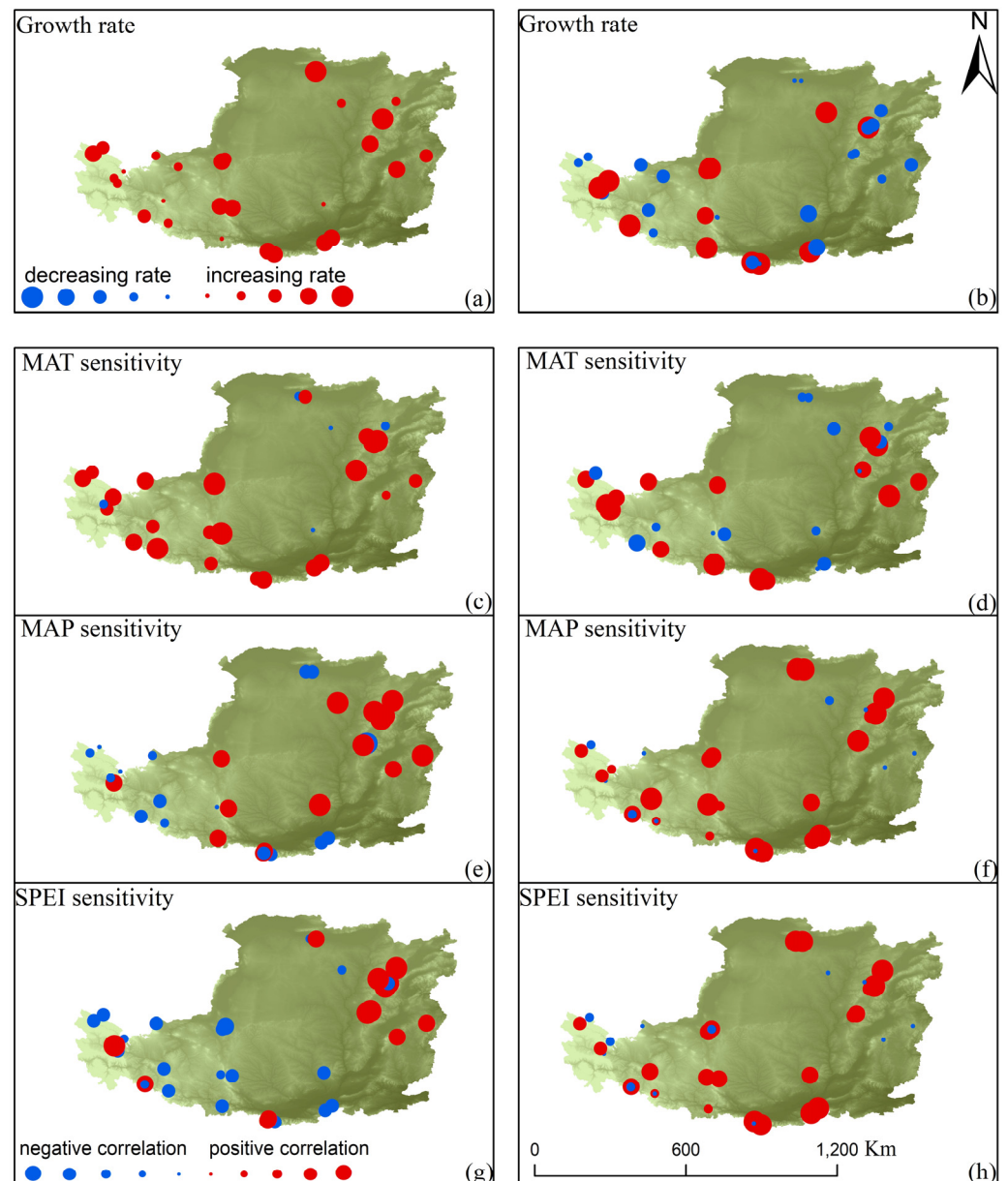


Figure 3. Spatial patterns of tree growth rates and climate sensitivity in two climate warming phases. MAT: temperature; MAP: precipitation. In graphs (a,b), the red and blue dots represent positive and negative tree growth rates, respectively, and the magnitude implies the size of the absolute value of the growth rate. In the (c–h) plot, the red and blue points represent the positive or negative response of tree growth sensitivity to climatic factors, respectively, and the magnitude implies the size of the absolute value of climate sensitivity.

3.3. Relationships between Tree Growth and Climate

The pattern of the correlations differed significantly between the two warming phases (Figure 4). During the first warming phase, tree growth had a correlation of 0.082 ± 0.206 with temperature, which changed to -0.131 ± 0.232 in the second warming phase. Additionally, the relationship between trees and both precipitation and SPEI shifted from negative (-0.021 ± 0.226 and -0.085 ± 0.224 , respectively) to positive (0.073 ± 0.225 and 0.077 ± 0.240 , respectively) correlations (Table S2). The tree ring index in the first warming phase exhibited a positive correlation with temperature during the previous and current year's growing seasons, while in the second warming phase, it demonstrated a strong negative correlation with temperature. In the second warming phase, tree ring

width was negatively correlated with temperature and progressively positively correlated with precipitation and SPEI, especially early in the previous year's growing season and late in the current year's growing season. Notably, common species like *A. fargesii*, *Larix chinensis*, and *Pinus tabulaeformis* exhibited a consistent pattern aligned with the overall trend (Figure S2).

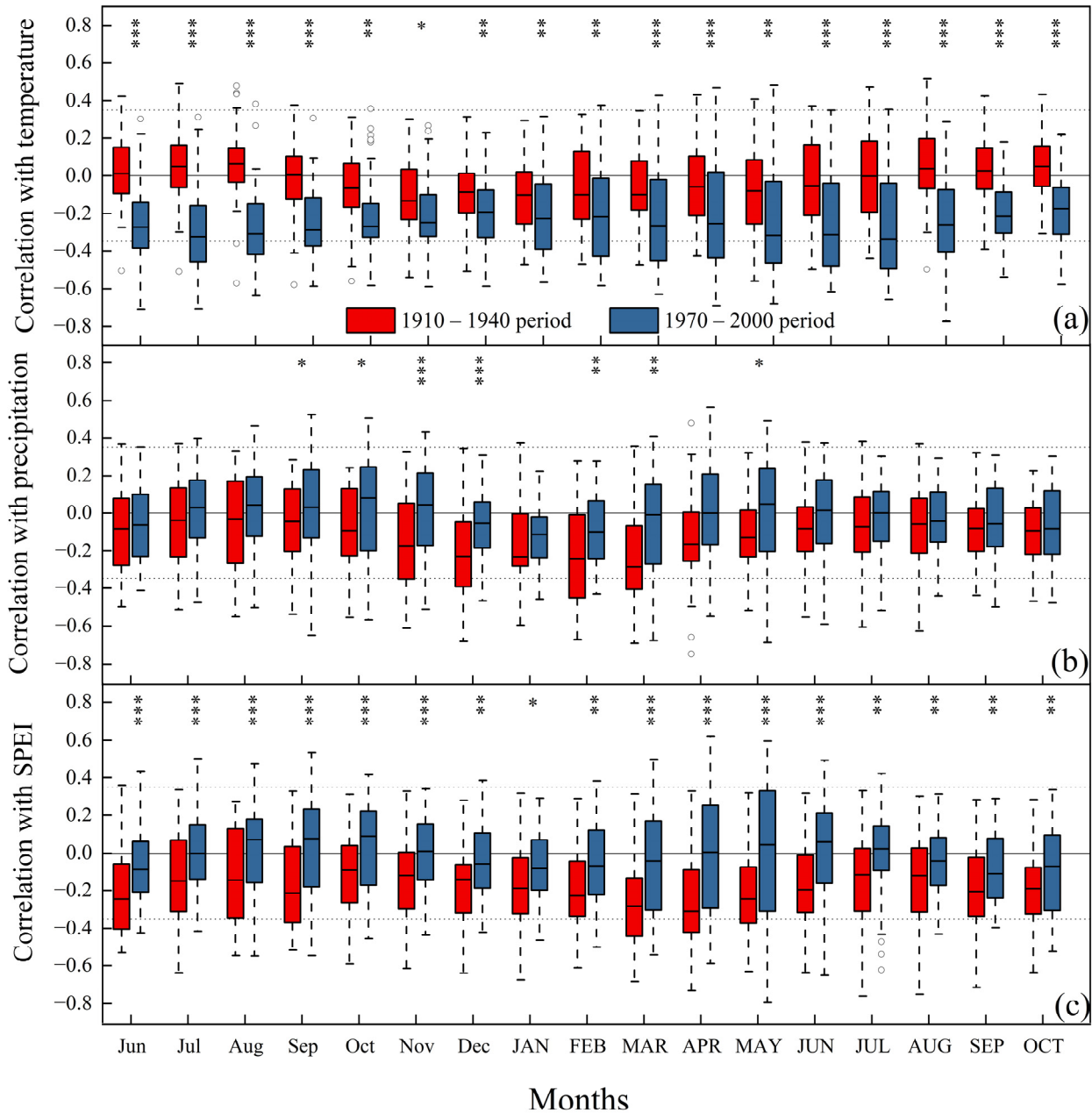


Figure 4. Correlation between tree rings index and climate in two warming phases. (a) Rings width and temperature correlation; (b) Rings width and precipitation correlation; (c) Rings width and SPEI correlation. Different asterisks indicate differences in climate sensitivity between the two warming phases, * $p < 0.05$, ** $p < 0.01$, and *** $p < 0.001$. Lowercase abbreviated months represent the previous year, while uppercase abbreviated months represent the current year. The circles indicate outliers.

4. Discussion

4.1. Trends in Climate and Tree Growth Rates

Climate warming trends were observed in the two phases in the Loess Plateau, accompanied by a decrease in precipitation and SPEI. Previous studies have documented

substantial increases in temperature indices in the Loess Plateau during 1961–2010, indicative of the warming trend in the region [22]. This temperature rise aligns with global warming trends and has persisted into the late 20th century [26,27]. Conversely, precipitation levels have shown a declining pattern, consistent with findings from other studies [28,29]. Anthropogenic warming has contributed to shifts in precipitation frequency across different intensity levels in most regions of the Loess Plateau between 1982 and 2015 [30]. MAP in the Loess Plateau has experienced cyclic fluctuations but overall displays a decreasing trend [31]. Moreover, a decreasing trend in spring and autumn precipitation has been detected in the region from 1961–2016 [28]. These long-term warming conditions have led to changes in precipitation patterns and frequencies, ultimately resulting in a relatively pronounced drying trend [24,32]. The shifts in precipitation frequency highlight the intricate interplay of local and global climate drivers, underscoring the complexity of the changes witnessed in the Loess Plateau. Notably, while most regions in Northern China have shown a wetter trend, the Loess Plateau has experienced increased aridity between 1961 and 2017 [33]. Future climate change scenarios suggest that this aridity trend may intensify in the region [34]. This alignment with global trends suggests that the Loess Plateau is not isolated from broader climate dynamics, and its vulnerability to climate change impacts becomes increasingly evident.

In the Loess Plateau, tree growth responded differently to the two warming phases in the 20th century. Specifically, tree growth rates were higher during the first warming phase but declined during the second phase, suggesting contrasting effects of these warming periods on tree growth. Similar findings have been reported in previous studies, such as the diminishing positive effects of spring temperatures on tree growth in the Shennongjia Mountains of China since the late 1970s [35]. *Picea likiangensis* in humid Southwestern China did not show a trend of decline under climate change, whereas spruce trees in water-limited areas would show growth decline [36]. These findings align with our data and indicate that tree growth is influenced by climate warming. Additionally, the effects of warming on tree growth rates vary across different regions and phases in China's diverse climate zones. For instance, while tree growth in humid Southwestern China did not exhibit a declining trend under changing climates, tree growth in the water-limited Loess Plateau experienced a decline [37]. These studies illustrate the need for area-specific assessments of the impacts of climate change on forest ecosystems, in particular climate change-induced changes in tree growth.

4.2. Variations of Tree Growth-Climate Relationships

The trends in tree growth rates during the two warming phases deviate from the consistent climate change trends observed. During the first warming phase, tree growth rates were higher, likely due to the relatively warm and humid climate with a small temperature increase. Additionally, trees did not experience significant drought stress during this phase. These findings suggest that moderate warming can be beneficial for tree growth. This perspective is supported by numerous studies conducted in different regions. For instance, in temperate regions, an increase in standard temperature has been shown to enhance tree photosynthesis rates [37,38]. In the Tibetan Plateau, warmer temperatures have significantly increased gross primary productivity through an increase in leaf area index [39]. It is likely that the initial temperature and aridity level stimulate physiological processes that promote tree growth, such as improving water use efficiency, enhancing light utilization, and increasing leaf area [40,41]. However, an ongoing trend of warming and drying persists during the secondary phase of warming. This extended pattern of warming–drying has the potential to negatively impact tree growth. Excessively high temperatures have been observed to hinder tree growth [42]. Elevated temperatures accelerate water evaporation, leading to soil drought. This phenomenon limits the availability of water and essential nutrients needed to sustain regular growth patterns in trees. Conversely, escalated drought stress also proves to be deleterious to tree growth. This notion is underscored by a study emphasizing that the prolonged elevation in climatic temperatures stands

as the primary catalyst for the decline in growth within *Pyrenean silver fir* forests [43]. The escalation in climatic temperatures has the potential to amplify tree mortality rates, particularly in warmer and drier regions [19]. Forests in semi-arid regions are more vulnerable to climate warming, further augmenting the frequency of loss in tree ring formations [44]. Collectively, these discoveries collectively emphasize a sustained trajectory of warming and drying as the chief instigator behind tree growth decline and even mortality.

The impact of climate warming on tree growth varies depending on the phase. In the first warming phase, temperature plays a dominant role, while in the second warming phase, water availability (precipitation and SPEI) becomes a significant factor. Previous studies have shown a notable decline in the correlation between tree growth and temperature in drylands between 1960 and 1990, indicating the presence of other factors limiting tree growth during the later warming phase [45]. However, the response of the tree ring index to precipitation and SPEI becomes more pronounced during this phase, suggesting that water availability becomes the primary limiting factor for tree growth. There are two possible reasons for this shift. Firstly, continued warming leads to increased evapotranspiration and a greater demand for water in the atmosphere [3,30]. This can be attributed to the combined effects of reduced tree growth rates, and accelerated evaporation rates driven by ongoing warming. Secondly, as warming and drying persist, precipitation patterns may undergo changes, resulting in reduced rainfall in drylands [46]. A previous study investigating the effects of temperature and precipitation trends on drought in the Loess Plateau region from 1961 to 2010 revealed that increased temperatures, coupled with limited reduction in precipitation, aggravated drought conditions in the area [22]. Therefore, the severe drought experienced during the later warming phase is the key factor for the shift in tree growth from temperature to water availability (precipitation and SPEI) in the Loess Plateau.

4.3. Response of Tree Radial Growth to Climate

Tree response to climate varies across months. The month-to-month climate change for the two warming phases is also shown in Figure S3. In the first warming phase, the temperature signal of tree ring data is most prominent in the current and previous year's growing season. However, in the second warming phase, the water signal of the tree rings index was mainly concentrated early in the current growing season and late in the previous growing season. In the first warming phase, warming promotes tree growth during the growing season. Therefore, trees are sensitive to temperature throughout the growing season. In the second warming phase, tree growth rates decreased, and tree chronology data were more sensitive to water availability. This implies that tree growth is under drought stress. Several studies have highlighted the importance of growing season precipitation in tree growth under drought conditions. For example, deciduous broadleaf forests in temperate regions primarily experience limited stand productivity due to current growing season water availability [47]. Likewise, in dryland ecosystems of the Silk Road Economic Belt, exacerbated drought enhanced the sensitivity of tree growth to early and mid-growing season precipitation [48]. These studies have demonstrated that with increasing drought severity, growing season precipitation plays an important role in tree growth. Similar findings supporting this idea have been observed in the Loess Plateau region. For instance, the radial growth of *Pinus armandii* in this area is positively correlated with precipitation throughout the growing season [25]. A controlled experiment to investigate the response of tree growth to precipitation found that supplemental water can greatly alleviate drought stress in trees [49]. Our data reveal that tree growth response to drought is weaker during the middle of the growing season compared to the early and late growing seasons. This is likely due to the concentration of precipitation in summer months in the Loess Plateau region, resulting in milder drought stress for trees in the middle of the growing season. Furthermore, an analysis of precipitation patterns in the Loess Plateau from 1965 to 2014 indicates spatial and temporal variability, with precipitation mainly concentrated in the summer months [50].

There is substantial evidence of forest decline due to warm drying, including the widespread decline of *Robinia Pseudoacacia* forests and soil desiccation [51–53]. This also suggests that climate warming has irreversible effects on forest ecosystems. It is important to note that our tree ring data are primarily derived from natural forests in the Loess Plateau region. However, it is essential to acknowledge that the Loess Plateau region has been implementing the Grain for Green program since 1999, resulting in large areas of plantation forests. These plantation forests may face substantial challenges in adapting to future climate conditions, necessitating a thoughtful reassessment of forest management strategies [54,55]. With further warming, drought stress in the Loess Plateau region is expected to increase and potentially subject forests to unprecedented drought stress [41,56]. Other water-limited regions are also at risk of facing similar challenges. Therefore, the management of forests to cope with climate change becomes of utmost importance. Certain adaptive forest management practices, such as thinning and land preparation, have already been implemented on the Loess Plateau with favorable outcomes [23,57,58]. Therefore, future forest management ought to not only take into account the effects of continued warming but also adopt scientific and effective management approaches. Furthermore, these findings have profound implications for carbon cycling and storage within ecosystems, ultimately influencing the global carbon balance. The response of forests to climate change in the Loess Plateau and other regions has far-reaching consequences for carbon sequestration and greenhouse gas emissions, making it imperative to address these issues within the broader context of climate mitigation and ecosystem management [43,59–61].

5. Conclusions

This study demonstrated how climate warming affects tree growth in two warming phases and tested our hypothesis that warming would alter tree growth rates and climate drivers in the Loess Plateau region. It was elucidated that in the two warming phases, temperature exhibited an increasing trend, while precipitation and SPEI demonstrated a decreasing trend. Tree growth rates changed from an increase to a subsequent decreasing trend during the two warming phases in the Loess Plateau. This shift in tree growth sensitivity moved from an initial responsiveness to temperature to a heightened sensitivity to drought stress. Moreover, the first warming phase temperatures promoted tree growth in the previous and current year's growing seasons, while the second warming phase drought stress was concentrated in the early and late growing seasons. Due to the projected intensification of warming, the Loess Plateau region is likely to experience increased aridity, amplifying stress on tree growth and potentially leading to forest decline and mortality. These findings carry practical implications for designing conservation strategies and forest management approaches, as well as for enhancing water resource management in dryland environments.

Supplementary Materials: The following supporting information can be downloaded at: <https://www.mdpi.com/article/10.3390/biology12101275/s1>, Table S1: Information about the 53 tree-ring chronologies in the Loess Plateau; Table S2: The comparison of tree ring indices, growth rate and climatic sensitivity during the two warming phases in the Loess Plateau; Figure S1: Trends in growth rates of different tree species in two warming phases; Figure S2: Correlation of tree rings index with temperature and precipitation for different tree species in two warming phases; Figure S3: Monthly changes in different climate factors during the two warming phases. All references in the supplementary material are in the text references [62–96].

Author Contributions: Conceptualization, Z.L. and Q.Z.; methodology, Z.L. and Q.Z.; software, S.F., H.G. and S.C.; investigation, Q.Z., S.F., H.G., S.C. and Z.L.; data curation, S.F., H.G. and S.C.; writing—original draft preparation, Q.Z.; writing—review and editing, Q.Z. and Z.L.; visualization, S.F. and H.G.; supervision, Z.L. All authors have read and agreed to the published version of the manuscript.

Funding: This work was funded by National Key Research Development Program of China (2022YFF0801802) and National Natural Science Foundation of China (42071125) to Z.L.; the Fundamental Research Program of Shanxi Province (20210302123333) to Q.Z.

Institutional Review Board Statement: Not applicable.

Informed Consent Statement: Not applicable.

Data Availability Statement: The data presented in this study are available on request from the corresponding author. The data are not publicly available yet as the authors are writing some other papers examining these data.

Acknowledgments: We would like to thank the anonymous reviewers and editors for their valuable comments that helped improve the current paper. We are very grateful to the projects for the funding provided to conduct this research work.

Conflicts of Interest: The authors declare no conflict of interest.

References

1. Scafetta, N. Discussion on climate oscillations: CMIP5 general circulation models versus a semi-empirical harmonic model based on astronomical cycles. *Earth Sci. Rev.* **2013**, *126*, 321–357. [[CrossRef](#)]
2. Fyllas, N.M.; Christopoulou, A.; Galanidis, A.; Michelaki, C.Z.; Dimitrakopoulos, P.G.; Fulé, P.Z.; Arianoutsou, M. Tree growth-climate relationships in a forest-plot network on Mediterranean mountains. *Sci. Total Environ.* **2017**, *598*, 393–403. [[CrossRef](#)] [[PubMed](#)]
3. Liu, H.; Park Williams, A.; Allen, C.D.; Guo, D.; Wu, X.; Anenkhonov, O.A.; Liang, E.; Sandanov, D.V.; Yin, Y.; Qi, Z.; et al. Rapid warming accelerates tree growth decline in semi-arid forests of Inner Asia. *Glob. Chang. Biol.* **2013**, *19*, 2500–2510. [[CrossRef](#)]
4. Roshani; Sajjad, H.; Kumar, P.; Masroor, M.; Rahaman, M.H.; Rehman, S.; Ahmed, R.; Sahana, M. Forest Vulnerability to Climate Change: A Review for Future Research Framework. *Forests* **2022**, *13*, 917. [[CrossRef](#)]
5. Cui, J.; Lian, X.; Huntingford, C.; Gimeno, L.; Wang, T.; Ding, J.; He, M.; Xu, H.; Chen, A.; Gentine, P.; et al. Global water availability boosted by vegetation-driven changes in atmospheric moisture transport. *Nat. Geosci.* **2022**, *15*, 982–988. [[CrossRef](#)]
6. Puntener, D.; Samonil, P.; Tikhomirov, D.; Danek, P.; Christl, M.; Rolecek, J.; Egli, M. Soil erosion rates during the Holocene continuity in a forest-steppe landscape. *Earth Surf. Process. Landforms* **2023**, *48*, 504–524. [[CrossRef](#)]
7. Brown, P.T.; Caldeira, K. Greater future global warming inferred from Earth's recent energy budget. *Nature* **2017**, *552*, 45–50. [[CrossRef](#)]
8. Saxe, H.; Cannell, M.G.R.; Johnsen, Ø.; Ryan, M.G.; Vourlitis, G. Tree and forest functioning in response to global warming. *New Phytol.* **2001**, *149*, 369–399. [[CrossRef](#)]
9. Zuidema, P.A.; Babst, F.; Groenendijk, P.; Trouet, V.; Abiyu, A.; Acuña-Soto, R.; Adenesky-Filho, E.; Alfaro-Sánchez, R.; Aragão, J.R.V.; Assis-Pereira, G.; et al. Tropical tree growth driven by dry-season climate variability. *Nat. Geosci.* **2022**, *15*, 269–276. [[CrossRef](#)]
10. Shi, S.; Liu, G.; Li, Z.; Ye, X. Elevation-dependent growth trends of forests as affected by climate warming in the southeastern Tibetan Plateau. *For. Ecol. Manag.* **2021**, *498*, 119551. [[CrossRef](#)]
11. Suarez, M.L.; Villalba, R.; Mundo, I.A.; Schroeder, N. Sensitivity of *Nothofagus dombeyi* tree growth to climate changes along a precipitation gradient in northern Patagonia, Argentina. *Trees* **2015**, *29*, 1053–1067. [[CrossRef](#)]
12. D'Orangeville, L.; Houle, D.; Duchesne, L.; Phillips, R.P.; Bergeron, Y.; Kneeshaw, D. Beneficial effects of climate warming on boreal tree growth may be transitory. *Nat. Commun.* **2018**, *9*, 3213. [[CrossRef](#)] [[PubMed](#)]
13. Gou, X.; Chen, F.; Jacoby, G.; Cook, E.; Yang, M.; Peng, J.; Zhang, Y. Rapid tree growth with respect to the last 400 years in response to climate warming, northeastern Tibetan Plateau. *Int. J. Climatol.* **2007**, *27*, 1497–1503. [[CrossRef](#)]
14. Li, X.; Piao, S.; Wang, K.; Wang, X.; Wang, T.; Ciais, P.; Chen, A.; Lian, X.; Peng, S.; Penuelas, J. Temporal trade-off between gymnosperm resistance and resilience increases forest sensitivity to extreme drought. *Nat. Ecol. Evol.* **2020**, *4*, 1075–1083. [[CrossRef](#)] [[PubMed](#)]
15. Liu, J.; Li, Z.-S.; Keyimu, M.; Wang, X.; Liang, H.; Feng, X.; Gao, G.; Fu, B.; Liang, E. Accelerated warming in the late 20th century promoted tree radial growth in the Northern Hemisphere. *J. Plant. Ecol.* **2023**, *16*, rtac077. [[CrossRef](#)]
16. Allen, C.; Breshears, D.D. Drought-induced shift of a forest–woodland ecotone: Rapid landscape response to climate variation. *Ecology* **1998**, *95*, 14839–14842. [[CrossRef](#)]
17. Allen, C.D.; Breshears, D.D.; McDowell, N.G. On underestimation of global vulnerability to tree mortality and forest die-off from hotter drought in the Anthropocene. *Ecosphere* **2015**, *6*, 1–55. [[CrossRef](#)]
18. Huang, M.; Wang, X.; Keenan, T.F.; Piao, S. Drought timing influences the legacy of tree growth recovery. *Glob. Chang. Biol.* **2018**, *24*, 3546–3559. [[CrossRef](#)]
19. Babst, F.; Bouriaud, O.; Poulter, B.; Trouet, V.; Girardin, M.P.; Frank, D.C. Twentieth century redistribution in climatic drivers of global tree growth. *Sci. Adv.* **2019**, *5*, eaat4313. [[CrossRef](#)]
20. Fu, B.; Liu, Y.; Meadows, M.E. Ecological restoration for sustainable development in China. *Natl. Sci. Rev.* **2023**, *10*, nwad033. [[CrossRef](#)]
21. Yu, Y.; Zhao, W.W.; Martinez-Murillo, J.F.; Pereira, P. Loess Plateau: From degradation to restoration. *Sci. Total Environ.* **2020**, *738*, 140206. [[CrossRef](#)] [[PubMed](#)]

22. Wang, Q.-x.; Fan, X.-h.; Qin, Z.-d.; Wang, M.-b. Change trends of temperature and precipitation in the Loess Plateau Region of China, 1961–2010. *Glob. Planet. Chang.* **2012**, *92–93*, 138–147. [[CrossRef](#)]
23. Fan, X.; Jiang, L.; Gou, J. Statistical downscaling and projection of future temperatures across the Loess Plateau, China. *Weather. Clim. Extrem.* **2021**, *32*, 1–12. [[CrossRef](#)]
24. Guo, M.Y.; She, D.X.; Zhang, L.P.; Li, L.C.; Yang, Z.L.; Hong, S. Attribution of trends in meteorological drought during 1960–2016 over the Loess Plateau, China. *J. Geogr. Sci.* **2021**, *31*, 1123–1139. [[CrossRef](#)]
25. Wang, A.; Gao, X.R.; Zhou, Z.Y.; Yang, H.; Zhao, X.H.; Wang, Y.M.; Li, M.; Zhao, X.N. Dynamic responses of tree-ring growth to drought over Loess Plateau in the past three decades. *Ecol. Indic.* **2022**, *143*, 109423. [[CrossRef](#)]
26. Ding, Z.Y.; Pu, J.; Meng, L.H.; Lu, R.J.; Wang, Y.Y.; Li, Y.P.; Dong, Y.Y.; Wang, S.Z. Asymmetric trends of extreme temperature over the Loess Plateau during 1998–2018. *Int. J. Climatol.* **2021**, *41*, E1663–E1685. [[CrossRef](#)]
27. Sun, Q.H.; Miao, C.Y.; Duan, Q.Y.; Wang, Y.F. Temperature and precipitation changes over the Loess Plateau between 1961 and 2011, based on high-density gauge observations. *Glob. Planet. Chang.* **2015**, *132*, 1–10. [[CrossRef](#)]
28. Wang, X.H.; Wang, B.T.; Xu, X.Y. Effects of large-scale climate anomalies on trends in seasonal precipitation over the Loess Plateau of China from 1961 to 2016. *Ecol. Indic.* **2019**, *107*, 105643. [[CrossRef](#)]
29. Gao, Y.; Feng, Q.; Liu, W.; Lu, A.G.; Wang, Y.; Yang, J.; Cheng, A.G.; Wang, Y.M.; Su, Y.B.; Liu, L.; et al. Changes of daily climate extremes in Loess Plateau during 1960–2013. *Quat. Int.* **2015**, *371*, 5–21.
30. Qiu, L.; Wu, Y.; Shi, Z.; Chen, Y.; Zhao, F. Quantifying the Responses of Evapotranspiration and Its Components to Vegetation Restoration and Climate Change on the Loess Plateau of China. *Remote Sens.* **2021**, *13*, 2358. [[CrossRef](#)]
31. Xu, X.M.; Huang, T. Spatiotemporal Trends and Variation of Precipitation over China’s Loess Plateau across 1957–2018. *Atmosphere* **2023**, *14*, 323. [[CrossRef](#)]
32. Zhao, Q.Z.; Ma, X.W.; Liang, L.; Yao, W.Q. Spatial-Temporal Variation Characteristics of Multiple Meteorological Variables and Vegetation over the Loess Plateau Region. *Appl. Sci.* **2020**, *10*, 1000. [[CrossRef](#)]
33. Yu, L.; Wu, Z.T.; Liu, Y.; Du, Z.Q.; Zhang, H. Does drought show a significant weakening trend from 1961 to 2017 in northern China? *Meteorol. Atmos. Phys.* **2022**, *134*, 31. [[CrossRef](#)]
34. Kong, D.X.; Miao, C.Y.; Duan, Q.Y.; Lei, X.H.; Li, H. Vegetation–Climate Interactions on the Loess Plateau: A Nonlinear Granger Causality Analysis. *J. Geophys. Res.* **2018**, *123*, 11068–11079. [[CrossRef](#)]
35. Zhao, Q.Y.; Xu, C.X.; An, W.L.; Liu, Y.C.; Xiao, G.Q.; Huang, C.J. Increasing tree growth in subalpine forests of central China due to earlier onset of the thermal growing season. *Agric. For. Meteorol.* **2023**, *333*, 109391. [[CrossRef](#)]
36. Wang, Y.; Zhang, Y.; Fang, O.Y.; Shao, X.M. Long-term changes in the tree radial growth and intrinsic water-use efficiency of Chuanxi spruce (*Picea likiangensis* var. *balfouriana*) in southwestern China. *J. Geogr. Sci.* **2018**, *28*, 833–844. [[CrossRef](#)]
37. Li, F.; Peng, Y.F.; Zhang, D.Y.; Yang, G.B.; Fang, K.; Wang, G.Q.; Wang, J.; Yu, J.C.; Zhou, G.Y.; Yang, Y.H. Leaf Area Rather Than Photosynthetic Rate Determines the Response of Ecosystem Productivity to Experimental Warming in an Alpine Steppe. *J. Geophys. Res. Biogeosci.* **2019**, *124*, 2277–2287. [[CrossRef](#)]
38. Nakamura, M.; Makoto, K.; Tanaka, M.; Inoue, T.; Son, Y.; Hiura, T. Leaf flushing and shedding, bud and flower production, and stem elongation in tall birch trees subjected to increases in aboveground temperature. *Trees* **2016**, *30*, 1535–1541. [[CrossRef](#)]
39. Linares, J.C.; Camarero, J.J. Growth patterns and sensitivity to climate predict silver fir decline in the Spanish Pyrenees. *Eur. J. For. Res.* **2012**, *131*, 1001–1012. [[CrossRef](#)]
40. Robbins, Z.J.; Xu, C.G.; Aukema, B.H.; Buotte, P.C.; Chitra-Tarak, R.; Fettig, C.J.; Goulden, M.L.; Goodsman, D.W.; Hall, A.D.; Koven, C.D.; et al. Warming increased bark beetle-induced tree mortality by 30% during an extreme drought in California. *Glob. Chang. Biol.* **2022**, *28*, 509–523. [[CrossRef](#)]
41. Valencia, E.; Quero, J.L.; Maestre, F.T. Functional leaf and size traits determine the photosynthetic response of 10 dryland species to warming. *J. Plant Ecol.* **2016**, *9*, 773–783. [[CrossRef](#)]
42. Crous, K.Y.; Drake, J.E.; Aspinwall, M.J.; Sharwood, R.E.; Tjoelker, M.G.; Ghannoum, O. Photosynthetic capacity and leaf nitrogen decline along a controlled climate gradient in provenances of two widely distributed Eucalyptus species. *Glob. Chang. Biol.* **2018**, *24*, 4626–4644. [[CrossRef](#)] [[PubMed](#)]
43. Sun, C.F.; Ma, Y.Y. Effects of non-linear temperature and precipitation trends on Loess Plateau droughts. *Quat. Int.* **2015**, *372*, 175–179. [[CrossRef](#)]
44. Taccoen, A.; Piedallu, C.; Seynave, I.; Gegout-Petit, A.; Gegout, J.C. Climate change-induced background tree mortality is exacerbated towards the warm limits of the species ranges. *Ann. For. Sci.* **2022**, *79*, 23. [[CrossRef](#)]
45. Liang, E.; Leuschner, C.; Dulamsuren, C.; Wagner, B.; Hauck, M. Global warming-related tree growth decline and mortality on the north-eastern Tibetan plateau. *Clim. Chang.* **2016**, *134*, 163–176. [[CrossRef](#)]
46. Liu, Z.J.; Liu, Y.S. Does Anthropogenic Land Use Change Play a Role in Changes of Precipitation Frequency and Intensity over the Loess Plateau of China? *Remote Sens.* **2018**, *10*, 1818. [[CrossRef](#)]
47. Helcoski, R.; Tepley, A.J.; Pederson, N.; McGarvey, J.C.; Meakem, V.; Herrmann, V.; Thompson, J.R.; Anderson-Teixeira, K.J. Growing season moisture drives interannual variation in woody productivity of a temperate deciduous forest. *New Phytol.* **2019**, *223*, 1204–1216. [[CrossRef](#)] [[PubMed](#)]
48. Hu, X.; Jiang, L.; Shi, F.; Li, X.; Zhang, S.; Zhao, Y.; Ma, Y.; Gao, Z.; Bai, Y. Intensified Drought Enhances Coupling between Vegetation Growth and Pregrowing Season Precipitation in the Drylands of the Silk Road Economic Belt. *J. Geophys. Res. Biogeosci.* **2021**, *126*, e2020JG005914. [[CrossRef](#)]

49. Xiao, S.C.; Peng, X.M.; Tian, Q.Y.; Zhu, G. Stem radial growth indicate the options of species, topography and stand management for artificial forests in the western Loess Plateau, China. *Sci. Cold Arid Reg.* **2019**, *11*, 226–238.
50. Tang, X.; Miao, C.; Xi, Y.; Duan, Q.; Lei, X.; Li, H. Analysis of precipitation characteristics on the loess plateau between 1965 and 2014, based on high-density gauge observations. *Atmos. Res.* **2018**, *213*, 264–274. [[CrossRef](#)]
51. Yao, L.; Fei, L.F.; Gui, S.; Liu, Q.S.; Liu, G.H. Remote sensing for monitoring on the health of artificial *Robinia Pseudoacacia* Forests in the Yellow River Delta. In Proceedings of the 2009 17TH International Conference on Geoinformatics, Fairfax, VA, USA, 12–14 August 2009; Volumes 1+2, p. 1088.
52. Chen, H.S.; Shao, M.G.; Li, Y.Y. Soil desiccation in the Loess Plateau of China. *Geoderma* **2008**, *143*, 91–100. [[CrossRef](#)]
53. Shangguan, Z.P. Soil desiccation occurrence and its impact on forest vegetation in the Loess Plateau of China. *Int. J. Sustain. Dev. World Ecol.* **2007**, *14*, 299–306. [[CrossRef](#)]
54. Chen, W.; Li, G.C.; Wang, D.L.; Yang, Z.; Wang, Z.; Zhang, X.P.; Peng, B.; Bi, P.S.; Zhang, F.J. Influence of the ecosystem conversion process on the carbon and water cycles in different regions of China. *Ecol. Indic.* **2023**, *148*, 110040. [[CrossRef](#)]
55. Wang, W.X.; Cui, C.F.; Yu, W.H.; Lu, L. Response of drought index to land use types in the Loess Plateau of Shaanxi, China. *Sci. Rep.* **2022**, *12*, 8668. [[CrossRef](#)] [[PubMed](#)]
56. Feng, T.J.; Wei, W.; Chen, L.D.; Cerda, A.; Yang, L.; Yu, Y. Combining land preparation and vegetation restoration for optimal soil eco-hydrological services in the Loess Plateau, China. *Sci. Total Environ.* **2019**, *657*, 535–547. [[CrossRef](#)]
57. Xu, L.H.; Cao, G.X.; Wang, Y.N.; Hao, J.; Wang, Y.H.; Yu, P.T.; Liu, Z.B.; Xiong, W.; Wang, X. Components of stand water balance of a larch plantation after thinning during the extremely wet and dry years in the Loess Plateau, China. *Glob. Ecol. Conserv.* **2020**, *24*, e01307. [[CrossRef](#)]
58. Cao, R.X.; Pei, Y.W.; Jia, X.X.; Huang, L.M. Rapid soil water recovery after conversion of introduced peashrub and alfalfa to natural grassland on northern China's Loess Plateau. *Can. J. Soil Sci.* **2020**, *100*, 302–313. [[CrossRef](#)]
59. Muller, C.; Stehfest, E.; van Minnen, J.G.; Strengers, B.; von Bloh, W.; Beusen, A.H.W.; Schaphoff, S.; Kram, T.; Lucht, W. Drivers and patterns of land biosphere carbon balance reversal. *Environ. Res. Lett.* **2016**, *11*, 044002. [[CrossRef](#)]
60. Manusch, C.; Bugmann, H.; Wolf, A. The impact of climate change and its uncertainty on carbon storage in Switzerland. *Reg. Environ. Chang.* **2014**, *14*, 1437–1450. [[CrossRef](#)]
61. Li, Y.Y.; Zhou, G.Y.; Liu, J.X. Different Growth and Physiological Responses of Six Subtropical Tree Species to Warming. *Front. Plant Sci.* **2017**, *8*, 1511. [[CrossRef](#)]
62. Cai, Q.; Liu, Y.; Lei, Y.; Bao, G.; Sun, B. Reconstruction of the March–August PDSI since 1703 AD based on tree rings of Chinese pine (*Pinus tabulaeformis* Carr.) in the Lingkong Mountain, southeast Chinese loess Plateau. *Clim. Past.* **2014**, *10*, 509–521. [[CrossRef](#)]
63. Cai, Q.F.; Liu, Y. Climatic response of Chinese pine and PDSI variability in the middle Taihang Mountains, north China since 1873. *Trees* **2013**, *27*, 419–427. [[CrossRef](#)]
64. Cai, Q.F.; Liu, Y. Climatic response of three tree species growing at different elevations in the Luliang Mountains of Northern China. *Dendrochronologia* **2013**, *31*, 311–317. [[CrossRef](#)]
65. Cai, Q.F.; Liu, Y.; Yang, Y.K.; Shi, J.F.; Sun, J.Y.; Wang, L. The reconstruction of tree-ring chronology and early spring (from February to March) precipitation information in Huanglong region, Shaanxi Province. *Mar. Geol. Quat.* **2005**, *25*, 133–139.
66. Chen, F.; Wang, H.; Chen, F.-H.; Yuan, Y.; Zhang, R.-B. Tree-ring reconstruction of July–May precipitation (AD 1816–2010) in the northwestern marginal zone of the East Asian summer monsoon reveals the monsoon-related climate signals. *Int. J. Climatol.* **2015**, *35*, 2109–2121. [[CrossRef](#)]
67. Chen, F.; Yuan, Y.J. May–June Maximum Temperature Reconstruction from Mean Earlywood Density in North Central China and Its Linkages to the Summer Monsoon Activities. *PLoS ONE* **2014**, *9*, e107501. [[CrossRef](#)]
68. Dang, H.S.; Jiang, M.X.; Zhang, Q.F.; Zhang, Y.J. Growth responses of subalpine fir (*Abies fargesii*) to climate variability in the Qinling Mountain, China. *For. Ecol. Manag.* **2007**, *240*, 143–150. [[CrossRef](#)]
69. Deng, Y.; Gou, X.H.; Gao, L.L.; Zhao, Z.Q.; Cao, Z.Y.; Yang, M.X. Aridity changes in the eastern Qilian Mountains since AD 1856 reconstructed from tree-rings. *Quat. Int.* **2013**, *283*, 78–84. [[CrossRef](#)]
70. Fang, K.Y.; Gou, X.H.; Chen, F.H.; Liu, C.Z.; Davi, N.; Li, J.B.; Zhao, Z.Q.; Li, Y.J. Tree-ring based reconstruction of drought variability (1615–2009) in the Kongtong Mountain area, northern China. *Glob. Planet. Chang.* **2012**, *80–81*, 190–197. [[CrossRef](#)]
71. Fang, K.Y.; Gou, X.H.; Chen, F.H.; Yang, M.X.; Li, J.B.; He, M.S.; Zhang, Y.; Tian, Q.H.; Peng, J.F. Drought variations in the eastern part of northwest China over the past two centuries: Evidence from tree rings. *Clim. Chang.* **2009**, *38*, 129–135. [[CrossRef](#)]
72. Fang, K.Y.; Wilmking, M.; Davi, N.; Zhou, F.F.; Liu, C.Z. An Ensemble Weighting Approach for Dendroclimatology: Drought Reconstructions for the Northeastern Tibetan Plateau. *PLoS ONE* **2014**, *9*, e86689. [[CrossRef](#)] [[PubMed](#)]
73. Gao, S.Y.; Lu, R.J.; Qiang, M.R.; Hasi, E.; Zhang, D.S.; Chen, Y.; Xia, H. Reconstruction of precipitation in the last 140 years from tree ring at south margin of the Tengger Desert, China. *Chin. Sci. Bull.* **2005**, *50*, 2487–2492. [[CrossRef](#)]
74. Liang, E.Y.; Shao, X.M.; Huang, L.; Wang, L.L. Indication of tree-ring on drought disasters in the 1920s in central and western China. *Prog. Nat. Sci.* **2004**, *14*, 111–116.
75. Li, Q.; Liu, Y.; Cai, Q.F.; Sun, J.Y.; Yi, L.; Song, H.M.; Wang, L. Reconstruction of annual precipitation since 1686 A.D. from Ningwu region, Shanxi Province. *Quat. Res.* **2006**, *26*, 99–1006.

76. Li, Q.; Liu, Y.; Nakatsuka, T.; Song, H.M.; McCarroll, D.; Yang, Y.K.; Qi, J. The 225-year precipitation variability inferred from tree-ring records in Shanxi Province, the North China and its teleconnection with Indian summer monsoon. *Glob. Planet. Chang.* **2015**, *132*, 11–19. [[CrossRef](#)]
77. Li, Q.; Liu, Y.; Song, H.M.; Yang, Y.K.; Zhao, B.Y. Divergence of tree-ring-based drought reconstruction between the individual sampling site and the Monsoon Asia Drought Atlas: An example from Guancen Mountain. *Sci. Bull.* **2015**, *60*, 1688–1697. [[CrossRef](#)]
78. Li, Y.J.; Gou, X.H.; Fang, K.Y.; Yang, T.; Deng, Y.; Man, Z.H. Reconstruction of precipitation of previous August to current June during 1821–2008 in the eastern Qilian Mountains. *J. Desert Res.* **2012**, *32*, 1393–1401.
79. Liu, Y.L.; Gou, X.H.; Zhang, F.; Yin, D.C.; Wang, X.J.; Xia, J.Q.; Li, Q.; Du, M.M. Effects of warming on radial growth of *Picea crassifolia* in the eastern Qilian Mountains, China. *Chin. J. Appl. Ecol.* **2021**, *32*, 3576–3584.
80. Liu, Y.; Tian, Q.H.; Song, H.M.; Sun, J.Y.; Linderholm, H.W.; Chen, D.; Cai, Q.F.; Ta, W.Y.; Lei, Y. Tree ring width based May–June mean temperature reconstruction for Huashan Mountain since A.D. 1558 and 20th century warming. *Quat. Sci.* **2009**, *29*, 888–895.
81. Li, Y.J.; Wang, S.Y.; Niu, J.J.; Fang, K.Y.; Li, X.L.; Li, Y.; Bu, W.L.; Li, Y.H. Climate-adial growth relationship of *Larix principis-rupprechtii* at different altitudes on Luya Mountain. *Acta Ecol. Sin.* **2016**, *36*, 1608–1618.
82. Qi, G.Z.; Bai, H.Y.; Meng, Q.; Zhao, T.; Guo, S.Z. Reconstruction of spring dry and wet changes in Taibai Mountain area bases on tree ring width. *Arid Land Geogr.* **2020**, *43*, 955–966.
83. Ren, J.L.; Liu, Y.; Song, H.M.; Ma, Y.Y.; Li, Q.; Wang, Y.C.; Cai, Q.F. The historical reconstruction of the maximum temperature over the past 195 year, Linxia region, Gansu Province—Based on the data from *Picea purpurea* Mast. *Quat. Sci.* **2014**, *34*, 1270–1279.
84. Song, H.M.; Liu, Y. PDSI variations at Kongtong Mountain, China, inferred from a 283-year *Pinus tabulaeformis* ring width chronology. *J. Geophys. Res. Atmos.* **2011**, *116*, 1–9. [[CrossRef](#)]
85. Song, H.M.; Mei, R.C.; Liu, Y.; Nievergelt, D.; Verstege, A.; Cherubini, P.; Liu, R.S.; Sun, C.F.; Li, Q.; Chen, L.; et al. Maximum July–September temperatures derived from tree-ring densities on the western Loess Plateau, China. *Int. J. Climatol.* **2021**, *41*, 779–790. [[CrossRef](#)]
86. Su, K.; Bai, H.Y.; Zhang, Y.; Huang, X.Y.; Qin, J. Reconstruction of precipitation history in Taibai Mountain of Qinling Mountains based on tree-ring width and meteorological data in recent 160 years. *Chin. J. Appl. Ecol.* **2018**, *37*, 1467–1475.
87. Sun, B.L.; Ma, L.; Liu, T.X.; Huang, X.; Zhou, Y. Temperature reconstruction based on 361 year old dendrochronology of *Platykladus orientalis* (L.) franco in the Wula Mountains, China. *Quat. Int.* **2021**, *583*, 94–102. [[CrossRef](#)]
88. Sun, C.F.; Liu, Y.; Song, H.M.; Mei, R.C.; Payomrat, P.; Wang, L.; Liu, R.S. Tree-ring—Based precipitation reconstruction in the source region of Weihe River, northwest China since AD 1810. *Int. J. Climatol.* **2018**, *38*, 3421–3431. [[CrossRef](#)]
89. Sun, Y.; Wang, L.L.; Chen, J.; Duan, J.P.; Shao, X.M.; Chen, K.L. Growth characteristics and response to climate change of *Larix Miller* tree-ring in China. *Sci. China-Earth Sci.* **2010**, *53*, 871–879. [[CrossRef](#)]
90. Wang, M.M.; Dai, J.H.; Bai, J.; Cui, H.T. Reconstruction of humidity changes from tree rings in Liupan Mountains area since 1900. *J. Palaeogeogr.* **2009**, *11*, 355–360.
91. Wang, Y.J.; Lu, R.J.; Ma, Y.Z.; Sang, Y.L.; Meng, H.W.; Gao, S.Y. Annual variation in PDSI since 1897 AD in the Tengger Desert, Inner Mongolia, China, as recorded by tree-ring data. *J. Arid Environ.* **2013**, *98*, 20–26. [[CrossRef](#)]
92. Wang, Y.J.; Ma, Y.Z.; Lu, R.J.; Sang, Y.L.; Meng, H.W.; Hua, F.C.; Man, Z.H. Reconstruction of mean temperatures of January to August since A.D. 1895 based on tree-ring data in the eastern part of the Qilian Mountains. *Quat. Sci.* **2009**, *29*, 905–912.
93. Wang, Y.J.; Ma, Y.Z.; Zheng, Y.H.; Lu, R.J.; Sang, Y.L.; Meng, H.W. Response of Tree-Ring Width of *Pinus tabulae* for mis to Climate Factors in Luoshan Mountains of Ningxia. *J. Desert Res.* **2009**, *29*, 971–976.
94. Zhang, Q.; Fang, O.Y. History of forest health from 1900 to 2012 in Xinzhou Prefecture, Shanxi Province. *Acta Ecol. Sin.* **2018**, *38*, 236–243.
95. Zhang, Y.X.; Wilmking, M.; Gou, X.H. Changing relationships between tree growth and climate in Northwest China. *Plant Ecol.* **2009**, *201*, 39–50. [[CrossRef](#)]
96. Zhu, X.L. Based on Tree Rings Study on the NDVI and SPEI Response of *Larix chensesis* in Qinling Mountains. Master Thesis, Northwest University, Xi’an, China, 2019.

Disclaimer/Publisher’s Note: The statements, opinions and data contained in all publications are solely those of the individual author(s) and contributor(s) and not of MDPI and/or the editor(s). MDPI and/or the editor(s) disclaim responsibility for any injury to people or property resulting from any ideas, methods, instructions or products referred to in the content.